

Exceptional running and turning performance in a mite

Samuel Rubin¹, Maria Ho-Yan Young², Jonathan C. Wright^{2,*},
Dwight L. Whitaker³, and A. N. Ahn⁴

¹Department of Chemical and Systems Biology, Stanford University School of Medicine, Stanford, CA 94305, USA, ²Department of Biology, Pomona College, Claremont, CA 91711, USA, ³Department of Physics, Pomona College, Claremont, CA 91711, USA, and ⁴Department of Biology, Harvey Mudd College, Claremont, CA 91711, USA

*Author for correspondence (jcw04747@pomona.edu)

Summary Statement

The mite *Paratarsotomus macropalpis* attains the highest relative speed and stride frequency documented for any animal. Kinematic analyses compare running in juveniles and adults, and gaits during straight runs and turning.

ABSTRACT

The Southern California endemic mite, *Paratarsotomus macropalpis*, was filmed in the field on a concrete substrate and in the lab to analyze stride frequency, gait, and running speed under different temperature conditions and during turning. At ground temperatures ranging from 45°C to 60°C, mites ran at a mean relative speed of $192.4 \pm 2.1 \text{ BL s}^{-1}$ (body lengths per second), exceeding the highest previously documented value for a land animal by 12.5%. Stride frequencies were also exceptionally high (up to 135 Hz), and increased with substrate temperature. Juveniles exhibited higher relative speeds than adults and possess proportionally longer legs, which allow for greater relative stride lengths. Although mites accelerated and decelerated rapidly during straight running ($7.2 \pm 1.2 \text{ ms}^{-2}$ and $-10.1 \pm 2.1 \text{ ms}^{-2}$, respectively), the forces involved were comparable to those found in other animals. *P. macropalpis* employs an alternating tetrapod gait during steady running. Shallow turns were accomplished by a simple asymmetry in stride length. During tight turns, mites pivoted around the tarsus of the inside third leg (L3), which thus behaved like a grappling hook. Pivot turns were characterized by a 42% decrease in turning radius and 40% increase in angular velocity compared to non-pivot turns. The joint angle amplitudes of the inner L2 and L3 were negligible during a pivot turn. While exceptional, running speeds in *P. macropalpis* approximate values predicted from inter-specific scaling relationships.

Key words: mite, relative speed, stride frequency, gait, turning

INTRODUCTION

Walking and running arachnids generally utilize variations on an alternating tetrapod gait, in which opposite legs are 180° out of phase in the stepping cycle and four legs (L1, L3, R2, R4, or L2, L4, R1, R3) contact the ground in stance phase at any given time (Spagna and Peattie, 2012). This gait structure, combined with the sprawled posture typical of most arachnid orders, provides both high static stability and maneuverability (Jindrich and Full, 1999; Weihmann, 2013). Although there is a growing body of work on spider locomotion and kinematics, much less is known about locomotion in mites (o. Acari). Mites offer interesting comparisons to other running arthropods, not only because of their small size and correspondingly high stride frequencies, but also because of the ability of many species to run rapidly and execute tight turns while traveling over extremely uneven substrates.

Mites attain some of the fastest relative speeds documented in the animal kingdom (Wu et al., 2010). Very small mites (<1 mg) represent some of the smallest running arthropods and, as such, they allow us to test whether or not models relating running speed and stride frequency to animal mass apply at lower mass extremes. Both relative speed (v_r) and stride frequency (f) scale negatively with body mass (M_b) (Alexander, 1982; Weyand et al., 2000; Iriarte-Diaz, 2002; Biewener, 2003; Wu et al., 2010). Dynamic similarity and the length-resonance relationship predict that $f \propto l^{-0.5}$, where l is leg length, as for a pendulum (Alexander and Jayes, 1973; Biewener, 2003; Hurlbert et al., 2008). Assuming isometric scaling of l and M_b ($l \propto M_b^{0.33}$), we can derive the predicted scaling of stride frequency and body mass as $f \propto M_b^{-0.17}$. Similarly, absolute speed (u) should scale as $M_b^{0.17}$ ($M_b^{-0.17} \times M_b^{0.33}$) and v_r should scale as $M_b^{-0.17}$ ($M_b^{0.17} / M_b^{0.33}$). Early work showed that this predicted scaling for v_r holds true for East African mammals (Pennycuik, 1975), and this was subsequently corroborated for other mammals (Garland, 1983). More recently, however, Iriarte-Diaz (2002) showed that mammals can be subdivided into smaller species (<30 kg) with a lower $v_r : M_b$ exponent of -0.09, and larger species with a considerably larger exponent (-0.46). Several factors may account for different exponent values and size-dependent changes in the exponent, including non-isometric scaling of limb length, metabolic power (Schmidt-Nielsen, 1984; Jones and Lindsted, 1993), and the interaction of metabolic power and dynamic similarity constraints (Hurlbert et al., 2008).

The negative scaling of v_r and f with body mass appears to hold true for other terrestrial taxa (Biewener, 2003; Full, 2011). However, scaling models based on vertebrates may not provide good predictors for behavior in very small animals below 1 g in mass. Here, predicted stride frequency may be limited by one or more components of muscle physiology and force generation: excitation-contraction coupling, actin-myosin cross-bridge cycling, and calcium-clearance required for muscle relaxation. Alternatively, the force-velocity trade-off for muscles could limit running speed and stride frequency at small sizes. Faster muscles not only generate less force as a result of faster cross-bridge cycling, as depicted in a typical force-velocity curve, but also tend to incorporate fewer contractile myofibrils. In ultrafast muscle fibers, the rapid cross-bridge cycling depends on high mitochondrial density to sustain the rapid ATP turnover, and the fast calcium clearance required for rapid relaxation depends on a large relative volume of sequestering sarcoplasmic reticulum (SR) (Appelt et al., 1991; Rome, 2006). Both mitochondria and SR compete for space with myofibrils, but how their relative volumes scale with muscle speed is unknown.

Paratarsotomus macropalpis (Banks, 1916) is an erythracarid mite occurring in the coastal sage scrub of Southern California (Otto, 2000). This species is known for its exceptional thermal tolerance (Wu and Wright, 2015) and locomotory performance (Wu et al., 2010), with relative speeds up to $133 BL s^{-1}$ and stride frequencies up to 111 Hz at 45°C. Here we build on previous work, using kinematic analysis of mites running on concrete substrates in the field to quantify running performance in undisturbed animals, and lab filming to analyze stride frequency and gait structure during straight running, acceleration and turning. We also analyze the effects of body size on stride frequency and relative speed among other fast-running species to see whether observed allometric scaling provides good predictions for running speed in *P. macropalpis*. Recently published data for arachnids (Spagna and Peattie, 2012) allow a comparison of relative speeds across multiple arachnid species, as well as among other terrestrial arthropods and vertebrates. In accordance with inter-specific scaling, we hypothesize that juvenile mites will utilize higher stride frequencies and attain higher relative speeds than their adult counterparts.

MATERIALS AND METHODS

Adult and juvenile *Paratarsotomus macropalpis* mites were filmed running in the lab and outdoors on concrete substrates in Claremont, CA, USA. Concrete served as a sufficiently light background to provide contrast for the mites during filming. Lab filming used a plastic Petri Dish or a larger enameled dish lined warmed with an incandescent lamp. Footage was captured using a high-speed CCD camera (Motion HG-100K, MotionXtra, RedLake, Tucson, AZ, USA) at 1000 frames s^{-1} . For outdoor filming, the camera was mounted vertically to a wheeled cart, allowing for easy movement while keeping it at a uniform distance from the ground surface. Calibration frames were recorded using a millimeter scale placed on the same substrate, which were used to compute body length and linear distances traveled. Ground surface temperatures were measured with a copper-constantan thermocouple in contact with the substrate adjacent to the mites' location.

All image processing and remedial motion analysis was performed with Tracker software (Open Source Physics, USA). To calculate speed and acceleration, mite bodies were manually digitized across sequences of 30 to 100 frames where mites ran in a straight path. Average speeds were also estimated by determining the straight-line distance between the start and end locations of the mites and dividing by the total running period. Within selected trials, the number of contacts between a specific limb tip (usually the second or third limb, depending on visibility) and the ground was divided by the running period to compute the animal's stride frequency (Hz). The number of individuals used to calculate mean values was different for each type of measurement because the footage from certain trials was not sufficiently clear to determine stride frequency by limb tracking, or because the footage lacked an absolute calibration slide.

Kinematic measures of mites and individual legs during initial acceleration, deceleration and turning were made in the lab in order to obtain sufficient resolution and image quality. Methods followed those described in Wu et al. (2010). Tracker software was used to measure angles of individual legs during the stride cycle relative to the longitudinal axis of the idiosoma in order to calculate stride angles from the beginning to the end of the aerial phase. During the stance phase, we measured the equivalent joint excursions from the time the tarsus contacted the ground surface to the time at which it was lifted. Changes in

orientation of animals during turns were similarly measured by tracking the longitudinal axis of the animal relative to a fixed grid. To compute leg tarsus speeds, the positions of individual leg tarsi in each frame were calculated from the x and y coordinates and distances tracked between successive frames.

Mites were collected for morphological measurements using an aspirator and preserved in 80% ethanol. Masses of mites were estimated assuming a hemispherical body shape using the following formula:

$$M_b = \rho \cdot (V_{sphere}/2) \quad (1)$$

where M_b represents body mass of a mite, ρ is density (1 mg mm⁻³ for *P. macropalpis* following Wu et al., 2010), and V_{sphere} is calculated assuming a mean radius ($r = 1/4 \times [\text{length} + \text{diameter}]$), and ignoring the legs. Calibrated frames with sufficiently resolved images were used to measure body lengths and diameters across the mites' idiosomae, yielding a mean estimated body mass of $268 \pm 18 \mu\text{g}$ (N = 7 individuals) for adult mites and $107 \pm 19 \mu\text{g}$ (N = 14 individuals) for juvenile mites. Body lengths and diameters as well as leg lengths were measured using a dissecting microscope equipped with a calibrated eyepiece reticle.

RESULTS

Running speed and stride frequency

P. macropalpis were field-active only at very high ground temperatures, ranging from 43–60°C. Juveniles and adults ran at similar absolute speeds (u) at 47.5 and 52.5°C, with a maximum recorded speed of 0.26 ms⁻¹ (Table 1). Relative speeds (v_r) in the field averaged $192.4 \pm 2.1 \text{ BL s}^{-1}$ (N = 32 individuals), with the fastest relative speed being 323 BL s⁻¹ for a juvenile mite. Comparing data for 47.5 and 52.5°C, v_r for juveniles was significantly higher than adults ($p < 0.01$; N = 24). Mites ran with an overall mean stride frequency (f) of $99.7 \pm 1.1 \text{ Hz}$ (N = 19), with a maximum recorded value of 135.0 Hz for a juvenile mite. Pearson correlation analysis shows that stride frequency increases significantly as a function of relative speed ($r = 0.561$; $p < 0.001$; N = 19). Log transformation of the two variables yields the following function:

$$f = 26 \cdot 8 \cdot v_r^{0.249} \quad (2)$$

The exponent of 0.249 is significantly smaller than unity ($p < 10^{-8}$, regression t-test), showing that increases in stride frequency only partially explain the higher relative speeds of juvenile mites.

Table 1. Mean running speeds and stride frequencies for adult mites (upper row for each temperature) and juvenile mites (lower row) recorded running freely in the field at different ground temperatures. Values show means \pm s.e.m. (N).

Ground Temperature [°C]	Absolute Speed, u [ms ⁻¹]	Relative Speed, v_r [BL s ⁻¹]	Stride Frequency, f [Hz]
47.5	0.140 \pm 0.005 (2)	133 \pm 4.6 (2)	72 \pm 9.5 (2)
	0.156 \pm 0.005 (4)	203 \pm 5.9 (6)	88 \pm 2.3 (5)
52.5	0.170 \pm 0.019 (5)	159 \pm 8.0(9)	104 \pm 5.0 (5)
	0.175 \pm 0.009 (4)	242 \pm 10.0 (7)	114 \pm 5.0 (5)
57.5	N/A	N/A	N/A
	0.120 \pm 0.009 (4)	194 \pm 9.2 (6)	110 \pm 4.8 (2)

The overall scaling relationship between relative speed and estimated body mass (kg) for juveniles and adults combined is:

$$v_r = 35.0 \cdot M_b^{0.102} \quad (3)$$

Despite the large differences in v_r , values for u and f did not differ significantly between juvenile and adult mites ($p = 0.6$, $p = 0.4$, respectively). In order to test whether juveniles achieve higher relative speeds with proportionally longer legs (and hence longer stride

lengths; Weyand et al., 2000), we analyzed the scaling of leg length (l) against body length for 21 preserved mites ranging in body length from 0.62 to 1.43 mm (Figure 1). Leg length increased progressively from anterior to posterior and for each of the four leg pairs, leg length increased significantly as a function of body length. The combined data for leg length show the following relationship to body length:

$$l = 1.26 \cdot BL^{0.641} \quad (4)$$

Relative speed and stride frequency both increased approximately linearly with temperature. Linear regression was used to calculate Q_{10} s for relative speeds between 45 and 55°C in adult *P. macropalpis*, which yielded a Q_{10} of 1.7 ($p = 0.03$; $N = 10$ individuals); data for juveniles did not yield a statistically significant Q_{10} . Stride frequencies for juveniles and adults combined increased with a Q_{10} of 1.6 ($p = 0.04$; $N = 17$ individuals).

Froude numbers (Fr) provide a dimensionless measure of speed normalized for body size and were calculated for combined mites at different temperatures using the formula (Alexander, 1982):

$$Fr = u^2 / (g BL) \quad (5)$$

where u = absolute running speed (ms^{-1}) and g = gravitational acceleration (9.81 ms^{-2}). Data from Table 1 yielded the following Fr values for the three mean temperatures: 1.56 (47.5°C), 2.03 (52.5°C), and 0.99 (57.5°C).

Starting and stopping

Acceleration achieved by mites during starting and stopping was determined by applying a linear regression to the calculated speeds between successive frames ($N = 10\text{--}20$ frames per mite). Juvenile and adult mites combined accelerated at an average of $7.2 \pm 1.2 \text{ ms}^{-2}$ ($N = 8$ individuals) and decelerated at an average of $-10.1 \pm 2.1 \text{ ms}^{-2}$ ($N = 5$ individuals) in the field. Given these mean values, mites will transition between a representative running speed of 0.150 ms^{-1} and rest in $15\text{--}20$ msec. Values measured in the lab were significantly smaller for both acceleration ($2.3 \pm 0.76 \text{ ms}^{-2}$; $N = 5$; $p < 0.002$) and deceleration ($0.98 \pm 0.30 \text{ ms}^{-2}$; $N = 5$; $p < 0.003$). The mean relative force (F/M) generated by a representative adult mite ($BL = 1 \text{ mm}$) during acceleration in the field was 0.52 g .

Braking forces are contributed by air resistance as well as muscle and elastic elements. We estimated the air resistance for a representative adult mite ($BL = 1.0 \text{ mm}$, ignoring the legs) running at 0.15 ms^{-1} at 50°C using the formula:

$$F_{\text{drag}} = k \cdot \eta \cdot BL \cdot u \quad (6)$$

where $k =$ a constant (3π for a spherical mite), $\eta =$ dynamic viscosity of air [$1.98 \times 10^{-5} \text{ N m}^{-2}\text{s}$ at 50°C], $BL =$ body length [m], and $u =$ absolute velocity [ms^{-1}] (Alexander, 1982). Calculated air resistance ($F_{\text{drag}} \approx 2.8 \times 10^{-8} \text{ N}$) is only about one percent of the force required for deceleration ($2.5 \times 10^{-6} \text{ N}$) and is therefore insignificant.

By tracking the position of the idiosoma and individual tarsi over time, we were able to analyze limb movements during steady running, as well as during acceleration, deceleration, and turning. A representative plot of tarsus speeds for the left legs during a straight run is shown in Figure 2 and the corresponding duty factors are given in Table 2. Opposite limbs move 180° out of phase. The near-synchrony of Legs 1 and 3 and Legs 2 and 4 shows that *P. macropalpis* utilizes an alternating tetrapod gait (L1R2L3R4 – L2R1L4R3, etc.). No other gait was observed during steady running. Legs 2 and 3 swing in a wide lateral arc. In contrast, the first and fourth leg pairs articulate in the sagittal plane and generate propulsive force by flexion and extension, respectively. The fourth pair of legs are the longest, approximately 1.8 times longer than the first pair, but display the lowest tip speeds and

longest aerial phase (and hence lowest duty factor) of any of the leg pairs. Their aerial phase typically extended slightly beyond that of the second pair. Changes in speed of the idiosoma were small and did not show an obvious pattern, although a small acceleration was sometimes observed following the onset of the stationary phase, resulting in an oscillation at twice the period of the gait cycle.

Although air resistance makes a minimal contribution to deceleration of the whole animal, it may represent a significant force slowing the legs during the aerial phase. To determine the drag force acting on the leg during the aerial (recovery) stroke, we modeled it as 3 cylinders of diminishing diameter (see Appendix 1). The drag behavior of a cylinder for a range of Reynolds numbers (Re) is given in White (2011). For our system Re varies from 0.23 to 0.37 for which drag per unit length (F') is approximated as

$$F' = C_D \cdot \rho \cdot u_l^2 \cdot \phi \quad (\text{Tomotika and Aoi, 1951}) \quad (7)$$

2

where C_D = Drag coefficient in air

ρ = Density of air

u_l = leg velocity

ϕ = leg diameter

This results in a calculated drag force of $1.1 \cdot 10^{-7}$ N

The force required to arrest the leg during deceleration in the recovery stroke can be estimated from the measured deceleration approximated from Fig. 2 (120 ms^{-2}) and an estimated leg mass of $1.9 \cdot 10^{-9}$ g. This gives a requisite deceleration force of $2.5 \cdot 10^{-7}$ N. The estimated drag force is approximately 40% of the force required to explain observed deceleration. Taking account of the rather low stride frequency for the animal in Fig. 2 (67 Hz), these calculations indicate that aerial drag acting on the leg during the recovery stroke is significant, and possibly the primary force arresting the leg at faster running speeds.

Table 2. Duty factors for the four leg pairs taken from a representative straight run comprising six stride cycles and including the left leg footage shown in Figure 2.

Leg pair	1	2	3	4
Mean Duty Factor	0.423	0.426	0.497	0.316
SEM	0.043	0.043	0.017	0.022
N	10	10	10	10

The distance covered per stride cycle was calculated from the ratio of running speed to stride frequency (u/f). Based on the mean values measured for adult mites at 52°C (Table 1), the approximate distance per cycle is 1.64 mm. Assuming a symmetrical gait, this will be equal to the average stride length per leg (Figure 3).

Turning

Mites executed two distinct types of turns: pivoting and non-pivoting. Pivot turns involved a highly stereotypical gait in which the animal pivoted around the tarsus of the inside (ipsilateral) Leg 3, which thus functioned like a grappling hook (Fig. 4; Movie 1). Non-pivot turns involved slower angular rotations and were accomplished by reductions in ipsilateral stride angles and proportional increases in contralateral stride angles (Table 3). Mites frequently turned through large angles when utilizing both types of turn; the mean changes in orientation for the turns analyzed were $103.4 \pm 48.8^\circ$ (mean \pm s.d.) for pivots and $102.0 \pm 38.6^\circ$ for non-pivots (Table 3). The turning radius in pivot turns (1.73 ± 0.05 mm) was narrowly defined, approximating the length of Leg 3 (1.71 mm \pm 0.023), and significantly smaller than for non-pivot turns (2.99 ± 0.31 mm; Table 3; $p < 0.05$). In accordance with their smaller turning radii, pivot turns had higher angular velocities ($\omega = 795 \pm 64$ deg sec⁻¹) when compared to non-pivot turns (567 ± 79 deg sec⁻¹; $p < 0.05$). The highest angular velocity measured during a pivot turn was 1253 deg sec⁻¹ and the highest during a non-pivot turn was 1040 deg sec⁻¹. Pivot and non-pivot turns did not differ in stride frequency or angular rotation per gait cycle (Table 3). Pivot and non-pivot turns also did not show any significant difference in stride frequency when compared to straight-running animals (N = 8) over a similar temperature range ($P > 0.1$).

Table 3. Summary kinematic data for mites filmed in the lab while using two different modes of turning. Student's t statistics from tests comparing the pivot and non-pivot means are given for each parameter (* $p < 0.05$; ** $p < 0.005$).

Turn type		Body Length (mm)	Turning Radius (mm)	Turning Radius (BL)	Degrees per gait cycle	Stride Frequency (Hz)	Time per gait cycle (msec)	Angular velocity (deg sec ⁻¹)
Pivot	<i>Mean</i>	1.14	1.73	1.53	30.9	26.5	41.5	795
(N = 11)	<i>s.e.m.</i>	0.028	0.048	0.032	1.31	2.57	3.68	64
Non-pivot	<i>Mean</i>	1.06	2.98	2.84	25.9	22.4	50.8	567
(N = 8)	<i>s.e.m.</i>	0.051	0.307	0.269	1.61	3.55	6.14	79
Student's t		ns	3.99 **	-	2.39 *	0.92 (ns)	1.28 (ns)	2.24*

Joint excursions for inner Legs 2 and 3 during pivot turns were negligible compared to the joint excursions for the outer Legs 2 and 3 during pivot turns, non-pivot turns, and straight running (Fig. 5). In pivot turns, the joint excursion for the ipsilateral legs is sharply reduced and not significantly different from zero; legs thus maintain a similar angle with respect to the idiosoma while the animal turns. Contralateral legs show large joint excursions, and in Leg 3 these are significantly larger than during straight running. During non-pivot turns, mites preserve the normal alternating tetrapod stepping pattern, but show a significant reduction in stride angles in the ipsilateral legs, and a corresponding increase in the contralateral stride angles, relative to a straight run.

The footfall patterns of a running mite, starting from rest and executing several turns, illustrate the alternating tripod gait used during straight running and the pivots about L3 during turning (Fig. 6). During initial acceleration (0 – 0.12 s), animals typically pulled with the first two leg pairs (R2 is not used in the footage in Fig. 6), while Legs 3 and 4 dragged passively behind for 3–5 gait cycles. No changes in footfall pattern were discernible during deceleration. Footfall patterns show clearly how animals rotated about the ipsilateral Leg 3 when executing a pivot turn; three such turns are included in Fig. 6. While pivoting around the tarsus of Leg 3, the duty factor of the ipsilateral Leg 2 was reduced. Because of the respective decrease and increase in ipsilateral and contralateral stride lengths, the limb tip speeds differed markedly, but duty factors of legs other than L3 and L2 changed minimally.

Interspecific scaling of v_r and f

To assess whether v_r in *P. macropalpis* is predicted from interspecific scaling, we examined v_r for fast runners including arachnids (Spagna and Peattie, 2012), mammals (Iriarte-Diaz, 2002) and several other taxa, ranging in size over 10 orders of magnitude (Figure 7; Appendix 2). Species were selected to comprise only fast runners (typically cursorial or ambush predators with high sprint speed), and drawn from as wide array of taxa as possible, minimizing over-representation of specific families. Thus, we include data for two of the fastest ants, despite data being available for multiple ant species (e.g. Hurlbert et al., 2008). The mean body length (BL) of juvenile mites filmed in the field on all calibrated footage was $711 \pm 43 \mu\text{m}$ ($N = 14$ individuals), and the mean BL for adults was $1005 \pm 23 \mu\text{m}$ ($N = 7$ individuals).

Mite speeds are closely predicted by scaling for the combined data ($\beta = 0.112$, or 0.103 excluding *P. macropalpis*) and by a regression for running arthropods excluding *P. macropalpis* ($\beta = 0.104$). These exponents also closely match the intraspecific exponent for *P. macropalpis* reported above ($\beta = 0.102$; Equation 2).

DISCUSSION

The mean relative speed of $192.4 BL s^{-1}$ measured for *P. macropalpis* in this study is the highest value for v_r currently documented for any terrestrial animal, exceeding the highest previously published value of $171 BL s^{-1}$ for the Australian tiger beetle, *Cicindela eburneola* (Kamoun and Hogenhout, 1996). The maximum stride frequency reported here, 135 Hz , is also the highest reported value for any weight-bearing muscle. The faster speeds relative to the lab measurements reported for this species by Wu et al. (2010) may be attributable in part to poor traction on the enamel substrate used for lab trials, but we believe they are also likely to be explained by injury sustained by animals during collection. Animals collected with an aspirator frequently had damaged legs and impaired mobility.

Juvenile *P. macropalpis* run at similar absolute speeds to adult mites, but consequently attain significantly higher relative speeds (Table 1). Comparing juveniles and adults, differences in stride frequency only partly explain the higher v_r in juveniles ($f \propto v_r^{0.249}$; Equation 2). The

requisite differences in stride length are consistent with the proportionally longer legs of juveniles (Equation 3). This ontogenetic change in relative stride length allows the smaller juveniles to run at similar absolute speeds to adults (Fig. 1). Adults and juveniles show similar Froude numbers, ranging from 0.99 to 2.03 depending on temperature, and conforming broadly to values published for other running arthropods (Biewener, 2003; Full, 2011) and for symmetrical gaits in tetrapods, consistent with the dynamic similarity hypothesis (Alexander and Jayes, 1983). For context, running mammals and lizards typically transition to asymmetric gaits at Froude numbers between 2 and 3.

Because mites were only field-active over a limited temperature range (substrate temperatures of 43–60°C), we had a smaller temperature range from which to assess the effect of temperature on running speed and stride frequency than in the lab trials used by Wu et al. (2010). However, our Q_{10} values for v_r (1.70) and f (1.60) calculated over 45–55°C show good agreement with the respective lab values for u (1.61) and f (1.59) calculated by Wu et al. (2010) for 40–50°C. Interestingly, neither u nor f showed the steep declines above 50°C reported by Wu et al. (2010). This decline in running performance in the prior study may be attributable to stress or injury sustained during field collection, but could also be a consequence of the rapid heating and cooling (between 22°C and experimental temperatures) imposed by the lab trials. Either way, while animals running freely in the field show a plateau and perhaps a modest decline in running performance above 55°C (Table 1), they are clearly able to maintain exceptional speeds at temperatures up to 60°C. Indeed, our second highest measured relative speed (301 $BL\ s^{-1}$) was for a juvenile at 60°C.

Despite the extremely high relative speeds and stride frequencies attained by *P. macropalpis*, allometric comparisons with other fast-running animals do not show the mite to be an outlier. The exceptional relative speeds documented for the tiger beetle *Cicindella eburneola* (Kamoun and Hogenhout, 2006) and the Ghost Crab *Ocypode ceratophthalma* (Burrows and Hoyle, 1973), present as much more dramatic outliers (Fig. 7; Appendix 2). Relative speeds (present study) and stride frequencies (Wu et al., 2010) for *P. macropalpis* are well predicted by interspecific scaling. The scaling exponent of 0.112 derived from our interspecific comparison underestimates mite v_r slightly, but almost exactly predicts mite speeds if these are adjusted using our Q_{10} values for a more representative temperature of 40°C (yielding v_r values of approximately 110 $BL\ s^{-1}$). Comparative data for arthropods yields a similar scaling exponent for v_r against M_b (0.104) and closely matches the intraspecific scaling exponent for

P. macropalpis (0.102). Taken together, allometric comparisons support dynamic similarity of *P. macropalpis* to other running animals. A caution should be applied, however, given the paucity of arthropod data, particularly for myriapods and crustaceans. More information is available for other arachnid orders (Spagna and Peattie, 2012), and these appear to show a steeper scaling of v_r with M_b , but as with other arthropods the data show considerable variance and lack representative species for several orders. Terrestrial runners are restricted to two major taxa – tetrapods and arthropods – with little overlap in mass ranges, which presents challenges to the application of phylogenetic comparative methods (Felsenstein, 1985; Garland et al., 2005; see also Rohlf, 2006). Future analyses accounting for independent origins of a running habit, and independent land colonization by different arthropod subphyla, may help to inform our understanding of v_r scaling.

P. macropalpis employs an alternating tetrapod gait as seen also in spiders (Ward and Humphreys, 1981; Biancardi et al., 2011) and several other arachnid orders (Spagna and Peattie, 2012). Although temporal resolution in our footage is limited by the very high stride frequencies (ca. 10 frames per stride cycle), duty factors approximate 0.5 for Leg 3, 0.42 for Legs 1 and 2, and somewhat lower (0.32) for Leg 4. This pattern is modified during acceleration, when the third and fourth leg pairs are dragged passively for 2–5 gait cycles. Based on our measurements of initial acceleration in the field and in the lab, this corresponds to the time required to attain a steady running speed (20–60 msec).

When executing tight turns, mites show a stereotypical gait, pivoting around the tarsus of the ipsilateral third leg. Such turns appear to involve the tarsus functioning as a grapple. The flexible distal part of the leg can be seen to stretch taut intermittently taut as the mite pivots, consistent with the anchor of the tarsal claws serving in the transfer of angular momentum (see Supplementary Video). In a shallow right turn, R3 follows the usual gait cycle but with reduced stride length and an increased duty factor, and may skip the aerial phase in adjacent gait cycles. Both pivot and non-pivot turns may involve very high angular velocities. The mean value for ω during pivot turns in the lab was 795 ± 64 deg sec⁻¹, which likely underestimates angular velocities at the higher stride frequencies exhibited in field conditions. Given the mites' ability to turn through 180° in 6–7 gait cycles, and assuming a stride frequency in the field of 100 Hz, they would be able to accomplish such a turn in less than 0.1 s. The peak angular velocity achieved by a pivoting mite in the current lab trials exceeded 1250 deg sec⁻¹. This pivoting, lateral turn by the mite is comparable in angular

velocity to the inversion behavior seen in the cockroach *Periplaneta* that uses a similar grappling hook mechanism to pivot vertically around the tarsus of a limb during escape ($>1200 \text{ deg sec}^{-1}$; Mongeau et al., 2012). Unlike *Periplaneta*, however, the mites continued to cycle their other limbs to move through the turn about the pivoted leg (Fig. 4; Table 3).

Although the pivoting (or grappling hook) mechanism has been described in inverting cockroaches and geckos (Mongeau et al., 2012), this use of a grappling hook during turning in *P. macropalpis* differs substantially from that described for most other arthropods. The octopodal gait in the tarantula *Grammostola mollicoma* uses a gait cycle where the ipsilateral legs are reversed during a sharp turn (Biancardi et al., 2011). Honey bees and dung beetles use similar ipsilateral gait reversals during tight turns (Zolotov et al., 1975; Frantsevich and Mokrushov, 1980). During more shallow turns, honey bees utilize similar gait adjustments to *P. macropalpis*, pivoting around the ipsilateral hind leg or relying on adjustments in stride length as the turning radius increases (Zolotov et al., 1975). During tight turns on a stick, squash bugs and stick insects also sometimes pivot slowly about the ipsilateral hind leg (Frantsevich and Cruse, 2005; Cruse et al., 2009). Other than for the ipsilateral Legs 2 and 3, stride frequency and duty factor do not change markedly during turning in *P. macropalpis* (Fig. 5), which is consistent with leg kinematics during turning in the spider *Metaphidippus hartfordi* (Land, 1972). Similar preservation of stride frequency and duty factor during turning is typical also for hexapods – for example, the fruit fly *Drosophila melanogaster* (Strauß and Heisenberg, 1990), 12 species of ants (Zollikofer, 1994), and the large cockroach *Blaberus discoidalis* (Jindrich and Full, 1999).

Mites, like several other arachnid orders, appear to lack leg extensor muscles in many or all of the joints and to depend on a threshold hemocoelic pressure to maintain leg extension (Schultz, 1989). This is apparent in *P. macropalpis* from the way in which the legs fold ventrally when animals are quiescent or dead, in a similar manner to those of spiders. Hydraulic Leg extension, well documented in spiders and other larger arachnids (Parry and Brown, 1959; Alexander, 1967; Schultz, 1991), is unlikely in *P. macropalpis* because the viscosity of hemocoelic fluid would not allow for movement in/out of the legs' narrow hemolymph canals at the rates required to sustain measured stride frequencies (Sensenig and Schultz, 2003). The measured lumen diameter of the basifemur, telofemur and patella in legs of an adult *P. macropalpis* is 40-60 μm . Assuming the viscous drag of hydraulic fluid follows Poiseuille's Law ($\text{drag} \propto r^4$), *P. macropalpis* legs would have about 10^7 times the

viscous drag of legs in a large arachnid such as *Aphonopelma*. Instead, it is probable that mites extend the main leg joints using the release of energy stored in loaded elastic sclerites (Sensenig and Schultz, 2003). Eliminating extensor muscles would confer the benefit of reducing leg mass and inertia and hence the kinetic energy required to sustain high stride frequencies (Full and Tu, 1991). Interestingly, there are only minor differences discernible in the kinetics of leg movements despite the fact that the active and recovery leg strokes likely employ fundamentally different mechanisms in the different leg pairs. Thus, in the extreme case, the first leg pair employs muscular shortening to flex the limb elements during the active stroke which pulls the animal forward. By contrast, in the fourth leg pair, the active stroke (stance phase) involves leg extension and probably employs the release of energy from loaded elastic sclerites, while muscle shortening flexes the limb during the recovery stroke. The storage and release of elastic energy in leg sclerites is clearly able to operate at the extreme frequencies (up to 135 Hz) observed. However, the reduced duty factor seen in the fourth legs, and the fact that the third and fourth pairs of legs are dragged passively during initial acceleration while the anterior legs pull the animal forward, may suggest that leg extension using elastic sclerites generates low propulsive force relative to muscular flexion.

During deceleration, mites did not show any clear change in gait pattern. Since air resistance is insufficient to explain observed deceleration, the main reaction forces employed in slowing are again probably imparted by the loading of elastic sclerites between the limb elements. At the cessation of the gait cycle on stopping, the idiosoma could be seen to rise and swing forward, representing the final transfer of forward momentum. A probable related function of elastic sclerites in *P. macropalpis* is passive energy absorption and dissipation (Sensenig and Schultz, 2003). Although we filmed animals on a concrete driveway, the species also occurs locally on open ground in coastal sage scrub habitats (Wu et al., 2010). The soils here comprise finely sorted alluvial sands and gravels and represent a very uneven terrain to an animal of ca. 1 mm. Passive shock-absorption of elastic elements may confer an important role in both stability and energy conservation, countering the constant shifting of a mite's center of mass when running on a typical substrate.

Measured values for acceleration and deceleration in *P. macropalpis*, although appearing very rapid, are comparable to values published for other running animals. Hunting cheetahs achieve accelerations between 0.1 and 1.0 g (Wilson et al., 2013) and the maximum acceleration achieved by Usain Bolt in the 100 m dash is 0.97 g (Hernández Gómez et al.,

2013). These similarities are consistent with the prediction that muscle work scales in proportion to muscle mass and body mass, allowing animals of different masses to attain comparable acceleration (Hill, 1950; Alexander, 1982).

Notwithstanding the exceptional relative speed and stride frequency shown by *P. macropalpis*, the good prediction of v_r and f from interspecific scaling (Fig. 7; Wu et al., 2010) indicates that the muscle contraction frequencies are likely optimized to exploit limb resonance for energy efficiency and are not limited by the force-velocity trade-off (Full, 2011). Because muscle force scales in proportion to cross-sectional area ($\propto M^{0.67}$), the relative muscle force per unit mass (F/M) scales as $M^{-0.33}$ ($M^{0.67}/M^1$), increasing as animals get smaller. Just as large animals need disproportionately large leg muscles to support their weight, very small animals can sacrifice muscle mass or the relative volume of myofibrils within a fiber. Even though *P. macropalpis* exhibits superfast weight-bearing muscles, the relative force they must generate is small by virtue of the mite's small mass. A larger portion of the mite's muscle volume could therefore be allocated to mitochondria and SR as in other ultra-fast (non-weight-bearing) muscles such as rattlesnake tail shaker muscles (Schaeffer et al., 1996) or the sonic swim bladder muscles in toadfish (Appelt et al., 1991; Rome et al., 1996). An open question is whether the predicted increase in stride frequency and relative speed for even smaller animals is ultimately limited by excitation-contraction coupling, calcium cycling, or other components of muscle performance. The fact that direct weight-bearing muscles can achieve the stride frequencies measured in juvenile mites (up to 135 Hz), involving contraction and relaxation times not exceeding 4 ms, demonstrates the extraordinary plasticity of muscle physiology.

In summary, *Paratarsotomus macropalpis* exhibits several exceptional locomotory attributes. In addition to attaining the fastest relative speed and stride frequency documented for running animals, the mites are capable of turning with extremely high angular velocities by utilizing the ipsilateral Leg 3 as a grappling hook. Allometric scaling of leg length during development results in proportionally longer legs juveniles and allows them to attain absolute and relative speeds comparable to those of adults.

LIST OF SYMBOLS AND ABBREVIATIONS

BL	body length
l	leg length
ϕ	leg diameter
f	stride frequency
g	acceleration due to gravity
M_b	body mass
F_{drag}	drag force
F'	drag force per unit length
k	constant that depends on body shape (3π for a sphere, such as a mite)
η	dynamic viscosity
C_D	drag coefficient
u	absolute speed
u_l	leg speed
v_r	relative speed
ρ	density
V_{sphere}	volume of a sphere
ω	angular velocity

ACKNOWLEDGEMENTS

The authors thank Ivo Ros for helpful discussions on data collection and software troubleshooting, as well as Jeremy Wright for his assistance with mite collection and filming. We are grateful to the feedback of two anonymous reviewers, including the suggestion to examine the role of air drag in slowing legs during the aerial phase. We thank the Departments of Biology and Physics at Pomona College, the Department of Biology at Harvey Mudd College, and the Keck Science Department.

AUTHOR COMPETING INTERESTS

We are not aware of any competing interests amongst the authors of this study that could affect the quality of our results.

AUTHOR CONTRIBUTIONS

Samuel Rubin and Maria Young performed experiments and all authors collaborated in data analysis. Samuel Rubin and Jonathan Wright prepared the manuscript. Jonathan Wright, Dwight Whitaker and Anna Ahn advised and oversaw the entire research endeavor and also helped edit the manuscript prior to submission.

FUNDING

This study was conducted with the support of the Howard Hughes Medical Institute Undergraduate Science Program awards 52006301 to Harvey Mudd College and 52007544 to the Claremont Colleges.

REFERENCES

- Alexander, R. McN.** (1967). Problems of limb extension in the scorpion, *Opisthophthalmus latimanus* Koch. *Trans. R. Soc. S. Africa* **37**, 165–181.
- Alexander, R. McN.** (1982). *Locomotion of Animals*. Bishopbriggs, Glasgow: Blackie & Son Limited.
- Alexander, R. McN. and Jayes, A.S.** (1983). A dynamic similarity hypothesis for the gaits of quadrupedal mammals. *J. Zool. (Lond.)* **201**, 135–152.
- Amaya, C.C., Klawinski, P.D. and Formanowicz, D.R.** (2001). The Effects of Leg Autotomy on Running Speed and Foraging Ability in Two Species of Wolf Spider, (Lycosidae). *Am. Mid. Nat.* **145**, 201-205.
- Appelt, D., Shen, V. and Franzini-Armstrong, C.** (1991). Quantitation of Ca ATPase, feet and mitochondria in superfast muscle fibres from the toadfish *Opsanus tau*. *J. Muscle Res. Cell Motil.* **12**, 543–552.
- Banks, N.** (1916). New Californian Mites. *Calif. J. Entomol. Zool.* **8**, 12–16.
- Biancardi, C.M., Fabrica, C.G., Polero, P., Loss, J.F. and Minetti, A.E.** (2011). Biomechanics of octopedal locomotion: kinematic and kinetic analysis of the spider *Grammostola mollicoma*. *J. Exp. Biol.* **214**, 3433–3442.
- Biewener, A. A.** (2003). *Animal Locomotion*. New York, NY: Oxford University Press.
- Burrows, M. and Hoyle, G.** (1973). The mechanism of rapid running in the ghost crab *Ocyropsis ceratophthalma*. *J. Exp. Biol.* **58**, 327–349.
- Clemente, C.J., Thompson, G.G. and Withers, P.C.** (2009). Evolutionary relationships of sprint speed in Australian varanid lizards. *J. Zool. (Lond.)* **278**, 270-280.
- Cruse, H., Ehmanns, I., Stübner, S., and Schmitz, J.** (2009). Tight turns in stick insects. *J. Comp. Physiol. A*, **195**, 299–309.
- Felsenstein, J.** (1985). Phylogenies and the comparative method. *Am. Nat.* **125**, 1-15.
- Foellmer, M.W., Marson, M., and Moya-Laraño, J.** (2011). Running performance as a function of body size, leg length and angle of incline in male orb-web spiders *Argiope aurantica*. *Evol. Ecol. Res.* **13**, 513-526.
- Franstevich, L.I. and Mokrushov, P.A.** (1980). Turning and righting in *Geotrupes* (Coleoptera, Scarabaeidae). *J. Comp. Physiol.* **136**, 279–289.
- Frantsevich, L. I. and Cruse, H.** (2005). Leg coordination during turning on an extremely narrow substrate in a bug, *Mesocercus marginatus* (Heteroptera, Coreidae). *J. Insect Physiol.*, **51**, 1092–1104.
- Full, R. J.** (2011). Invertebrate locomotor systems. *Compr. Physiol.* **30**, 853–930.

- Full, R.J. and Tu, M.S.** (1991). Mechanics of six-legged runners. *J. Exp. Biol.* **148**, 129–146.
- Garland, T.** (1983). The relation between maximal running speed and body mass in terrestrial mammals. *J. Zool.* **199**, 157–170.
- Garland, T., Bennett, A.F., and Rezende, E.L.** (2005). Phylogenetic approaches in comparative physiology. *J. Exp. Biol.* **208**, 3015–3035.
- Gorb, S.N. and Barth, F.G.** (1994). Locomotion behavior during prey capture of a fishing spider *Dolomedes plantarius* (Aranae: Araneidae): galloping and stopping. *J. Arachnology* **22**, 89–93.
- Hernández Gómez, J.J., Marquina, V. and Gómez, R.W.** (2013). On the performance of Usain Bolt in the 100m sprint. *Eur. J. Phys.* **34**, 1227–1233.
- Hill, A.V.** (1950). The dimensions of animals and their muscular dynamics. *Sci. Prog., Lond.* **38**, 209–30.
- Hurlbert, A.H., Ballantyne, F. and Powell, S.** (2008). Shaking a leg and hot to trot: the effects of body size and temperature on running speed in ants. *Ecol. Entomol.* **33**, 144–154.
- Iriarte-Díaz, J.** (2002). Differential scaling of locomotor performance in small and large terrestrial mammals. *J. Exp. Biol.* **205**, 2897–2908.
- Irschick, D.J. and Jayne, B.C.** (1999). Comparative three-dimensional kinematics of the hindlimb for high-speed bipedal and quadrupedal locomotion of lizards. *J. Exp. Biol.* **202**, 1047–1065.
- Jindrich, D.L. and Full, R.J.** (1999). Many-legged maneuverability: dynamics of turning in hexapods. *J. Exp. Biol.* **202**, 1603–1623.
- Jones, J.H. and Lindstedt, S.L.** (1993). Limits to maximal performance. *Ann. Rev. Physiol.* **55**, 547–569.
- Kamoun, S. and Hogenhout, S. A.** (1996). Flightlessness and rapid terrestrial locomotion in tiger beetles of the *Cicindela* L. Subgenus *Rivacindela* van Nidek from saline habitats of Australia (Coleoptera: Cicindelidae). *Coleopt. Bull.* **50**, 221–230.
- Land, M.** (1972). Stepping patterns made by jumping spiders during turns mediated by the lateral eyes. *J. Exp. Biol.* **56**, 15–40.
- Manton, S. M.** (1965). The evolution of arthropod locomotory mechanisms. Part 8. *J. Linn. Soc. Lond., Zoology* **46**(306–307), 251–483.

- Nicolson, S.W., Bartholemew, G.A. and Seeley, M.K.** (1984). Ecological correlates of locomotion speed, morphometrics and body temperature in three species of Namib Desert tenebrionid beetles. *S. Afr. J. Zool.* **19**, 131-134.
- Otto, J. C.** (2000). A cladistic analysis of Erythracarinae (Acarina: Prostigmata: Anystidae), with description of a new genus. *Syst. Entomol.* **25**, 447-484.
- Parry, D.A. and Brown, R.H.J.** (1959). The hydraulic mechanism of the spider leg. *J. Exp. Biol.* **36**, 423-433.
- Pennycuik, C.J.** (1975). On the running of the gnu (*Connochaetes taurinus*) and other animals. *J. Exp. Biol.* **63**, 775-799.
- Punzo, F.** (1998). *The Biology of Camel Spiders (Arachnida, Solifugae)*. Springer, New York.
- Rohlf, F.J.** (2006). A comment on phylogenetic correction. *Evolution* **60**, 1509-1515.
- Rome, L. C., Syme, D. A., Hollingworth, S., Lindstedt, S. L. and Baylor, S. M.** (1996). The whistle and the rattle: the design of sound producing muscles. *Proc. Nat. Acad. Sci. USA.* **93**, 8095-8100.
- Rome, L.C.** (2006). Design and function of superfast muscles: new insights into the physiology of skeletal muscle. *Ann. Rev. Physiol.* **68**, 193-221.
- Schaeffer, P. J., Conley, K. E. and Lindstedt, S. L.** (1996). Structural correlates of speed and endurance in skeletal muscle: the rattlesnake tailshaker muscle. *J. Exp. Biol.* **198**, 351-358.
- Schmidt-Nielsen, K.** (1984). *Why is Animal Size so Important?* Cambridge University Press, Cambridge, U.K.
- Schultz, J.W.** (1989). Morphology of locomotor appendages in Arachnida: evolutionary trends and phylogenetic implications. *Zool. J. Linn. Soc.* **97**, 1-56.
- Schultz, J.W.** (1991). Evolution of locomotion in Arachnida: the hydraulic pressure pump of the giant whipscorpion, *Mastigoproctus giganteus* (Uropygi). *J. Morphol.* **210**, 13-31.
- Sensenig, A.T. and Schultz, J.W.** (2003). Mechanics of cuticular elastic energy storage in leg joints lacking extensor muscles in arachnids. *J. Exp. Biol.* **206**, 771-784.
- Spagna, J.C., Valdivia, E. and Mohan, V.** (2011) Gait characteristics of two fast-running spider species (*Hololena adnexa* and *Hololena curta*), including an aerial phase (Araneae: Agelenidae). *J. Arachnology* **39**,1-8.
- Spagna, J.C. and Peattie, A.M.** (2012). Terrestrial locomotion in arachnids. *J. Insect Physiol.* **58**, 599-606.

- Strauß, R. and Heisenberg, M.** (1990). Coordination of legs in *Drosophila melanogaster* during straight walking and turning. *J. Comp. Physiol. A* **167**, 403–412.
- Tomotika, S. and Aoi, S.** (1951). An expansion formula for the drag on a circular cylinder moving through a viscous fluid at small Reynolds numbers. *Quart. J. Mech. Appl. Math.* **4**, 401-406.
- Ward, T.M. and Humphreys, F.W.** (1981). Locomotion in Burrowing and Vagrant Wolf Spiders (Licosidae). *J. Exp. Biol.* **92**, 305–321.
- Wehner R.** (1983). Taxonomie, Funktionsmorphologie und Zoogeographie der saharischen Wüstenameise *Cataglyphis fortis* (Forel 1902) *stat. nov. Senckenbergiana Biol.* **64**, 89–132.
- Weihmann, T.** (2013). Crawling at high speeds: steady level locomotion in the spider *Cupiennius salei* – global kinematics and implications for center of mass dynamics. *PLoS ONE* **8**: e65788.
- Weyand, P. G., Sternlight, D. B., Bellizzi, M. J. and Wright, S.** (2000). Faster top running speeds are achieved with greater ground forces not more rapid leg movements. *J. Appl. Physiol.* **89**, 1991–1999.
- White, F.M.** (2011). *Fluid Dynamics*. Seventh Edition. McGraw-Hill, New York, NY.
- Wilson, A. M., Lowe, J. C., Roskilly, K., Hudson, P. E., Golabek, K. A. and McNutt, J. W.** (2013). Locomotion dynamics of hunting in wild cheetahs. *Nature* **498**, 185–189.
- Wittlinger, M., Wehner, R. and Wolf, H.** (2007). The desert ant odometer: a stride integrator that accounts for stride length and walking speed, *J. Exp. Biol.* **210**, 198-207.
- Wu, G.C. and Wright, J.C.** (2015). Exceptional thermal tolerance and water resistance in the mite *Paratarsotomus macropalpis* (Acarina: Anystidae: Erythracarinae). *J. Insect Physiol.* **82**, 1-7.
- Wu, G. C., Wright, J. C., Whitaker, D. L. and Ahn, A. N.** (2010). Kinematic evidence of superfast locomotory muscle in two species of teneriffiid mites. *J. Exp. Biol.* **213**, 2551–2558.
- Zollikofer, C.P.** (1994). Stepping patterns in ants. I. Influence of speed and curvature. *J. Exp. Biol.* **192**, 95–106.
- Zolotov, V., Frantsevich, L., and Falk, E-M.** (1975). Kinematik der phototakischen Drehung bei der honigbiene *Apis mellifera* L. *J. Comp. Physiol.* **97**, 339–353.

Figures

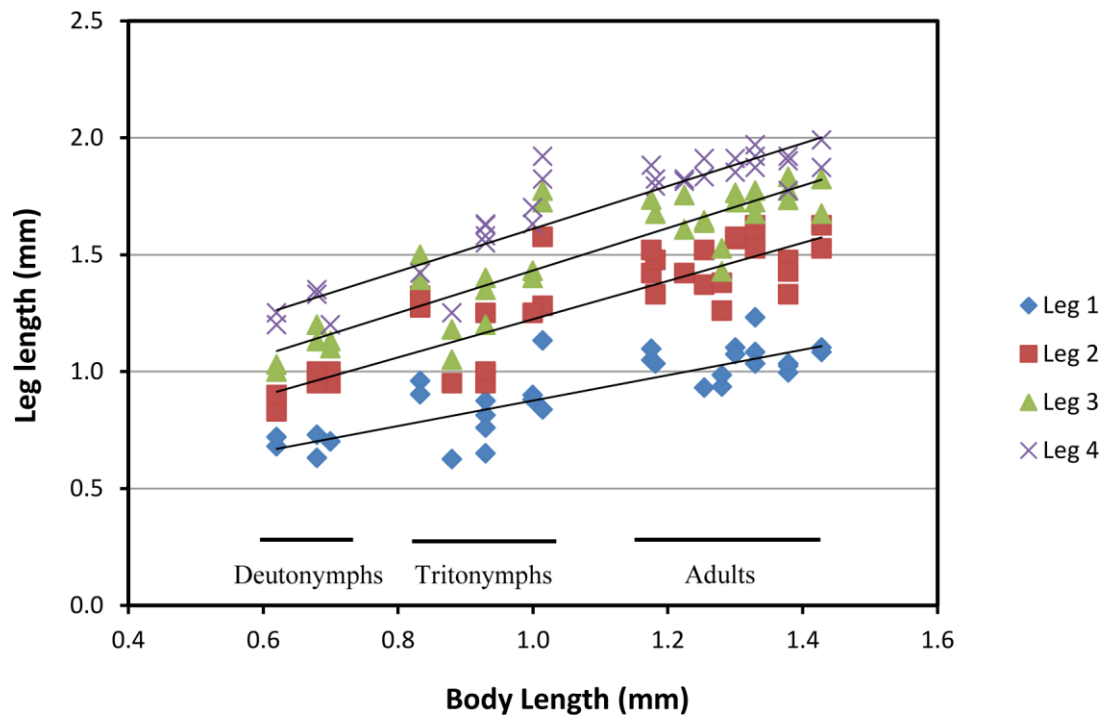


FIG. 1. Measured leg lengths for 21 preserved specimens of *P. macropalpis* as a function of body (idiosoma) length. All four leg pairs scale non-isometrically with body length, with juveniles having proportionally longer legs.

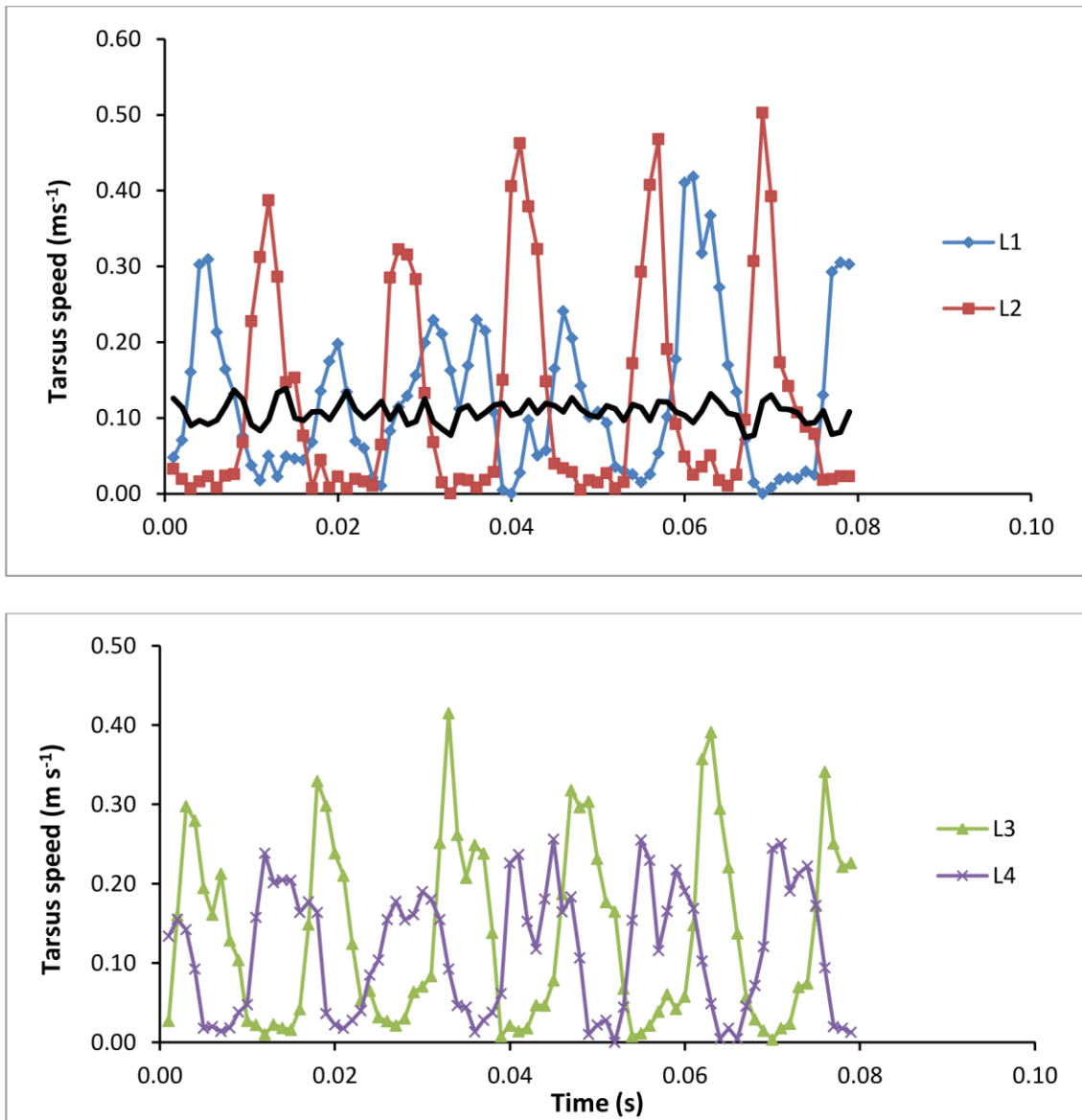


FIG. 2. Tarsal speeds of the four left legs in a representative adult *P. macropalpis* measured during an 80 msec straight run. The upper plot shows Legs 1 and 2, with the black line showing the corresponding speed of the body measured at the center of the idiosoma. The lower plot shows Legs 3 and 4.

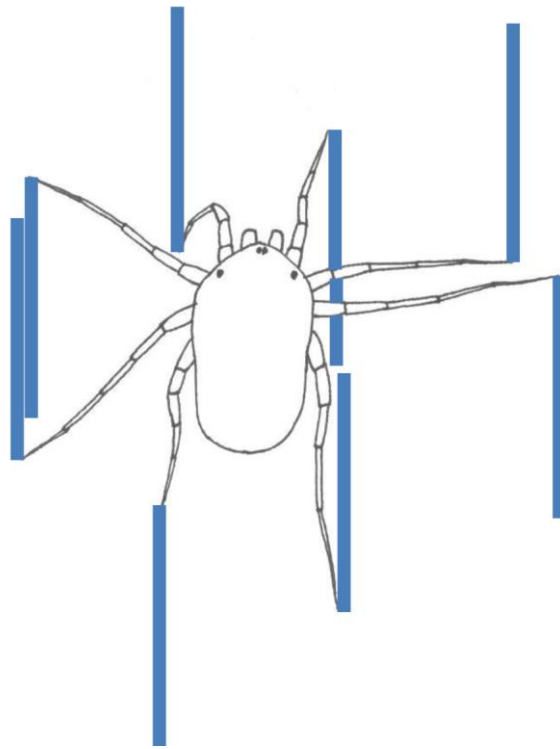


FIG. 3. Gait pattern in *P. macropalpis* sketched from video footage and showing the limbs close to the extremes of the stride excursion. The blue, vertical bars show the approximate longitudinal excursions of each of the 8 legs during the previous (right L1, L3; left L2, L4) and next (left L1, L3; right L2, L4) aerial phase. Opposite limbs are approximately 180° out of phase.

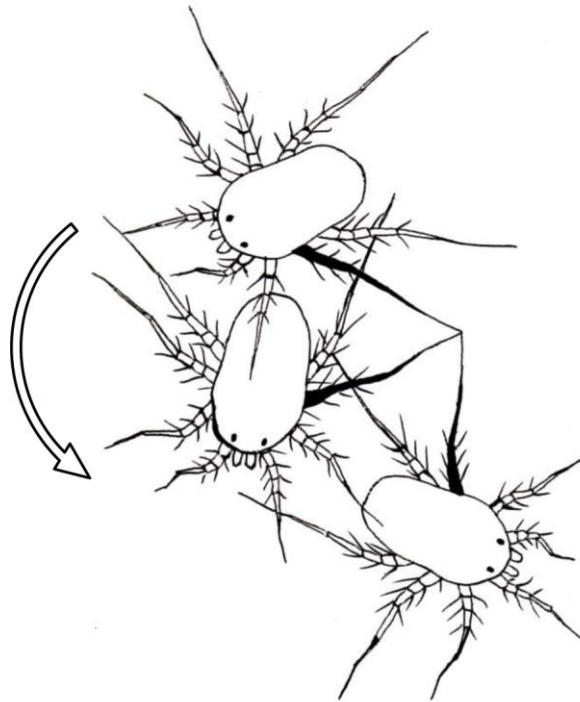


FIG. 4. Diagram of *Paratarsotomus macropalpis* executing a tight left turn through 120° while pivoting about L3 (shown in black). The three images are sketched from individual frames of video footage and separated in time by approximately 60 msec. Most of the long setae on the legs are omitted for clarity. Although the illustration only shows three positions of the mite, this turn encompassed 3.5 gait cycles. The arrow shows the direction of the turn and a scale length of 2 mm.

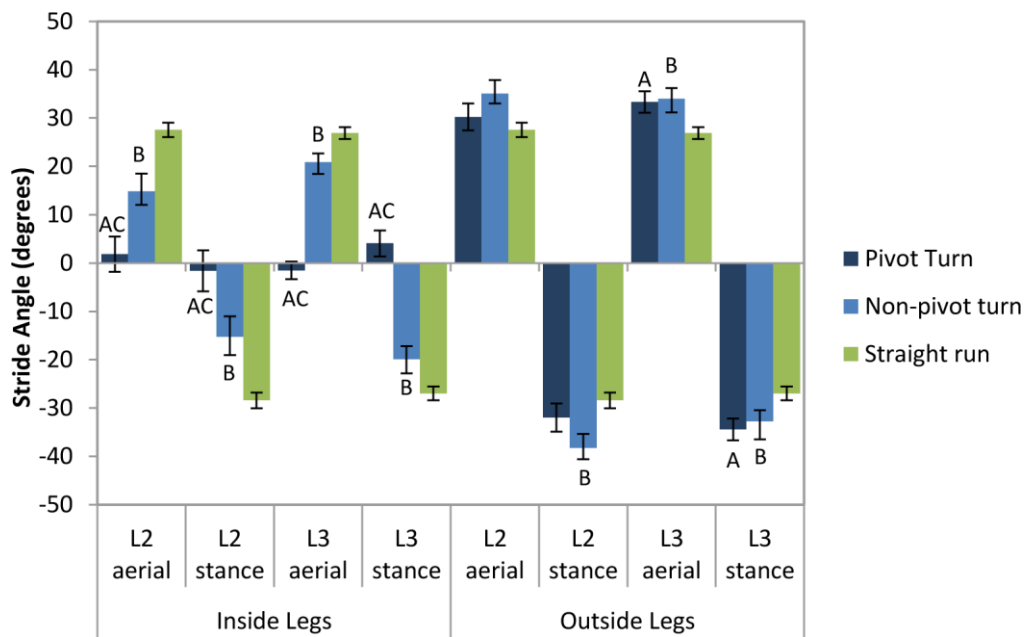


FIG. 5. Stride angles of Leg 2 (L2) and Leg 3 (L3) for the aerial (recovery) and stance (active) stroke during pivot turns, non-pivot turns, and straight running. Bars show ± 1 s.e.m. Inside (ipsilateral) and outside (contralateral) angles for a given leg are the same in the straight runs.

Because the inside L3 remains in stance during a pivot turn, there was no aerial phase; the angle shown is the equivalent angular change (joint excursion) measured during the recovery stroke. The inside L2 and L3 remained at similar angles relative to the body during pivot turns while outside stride angles increased relative to a straight run. Non-pivot turns involved an increase in stride angles of the outside L2 and L3, and a decrease in the equivalent inside stride angles, relative to a straight run, but preserved the basic gait pattern. Means were derived from analysis of 5 adult mites in each case, using 2–6 gait cycles per animal. Letters denote significant differences ($p < 0.05$) using a 2-way ANOVA to compare stride angles during pivot turns and straight runs (A), non-pivot turns and straight runs (B), and pivot and non-pivot turns (C). $N = 11$ – 21 for turns and 28 – 38 for straight runs.

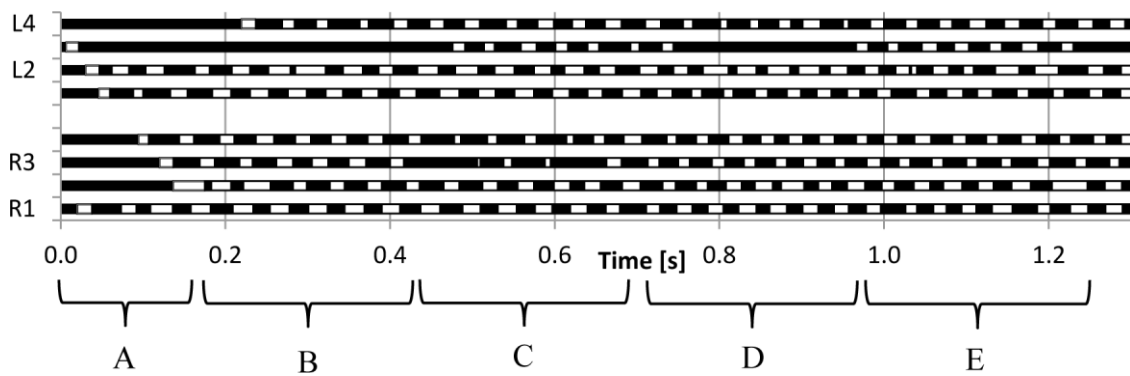


FIG. 6. Footfall diagram for a representative *P. macropalpis* accelerating from rest followed by a period of running and turning in the lab. Each horizontal bar depicts the footfall pattern of a single limb with black showing the stance (ground) phase and white showing the swing (aerial) phase. Bracketed periods denote specific locomotory patterns:

- A. Initial acceleration: the mite pulls at the ground with the first two leg pairs. The rear two pairs are dragged briefly before adopting the alternating tetrapod gait cycle.
- B. Left turn, pivoting around L3. The gait cycle is essentially preserved, but stride length is reduced in L2 to enable the turn.
- C. Right turn, pivoting about R3. Contact between R3 and the ground is broken briefly several times, resulting in a shallower turn.
- D. Left turn pivoting about L3.
- E. Straight run showing the stereotypical alternating tetrapod gait cycle.

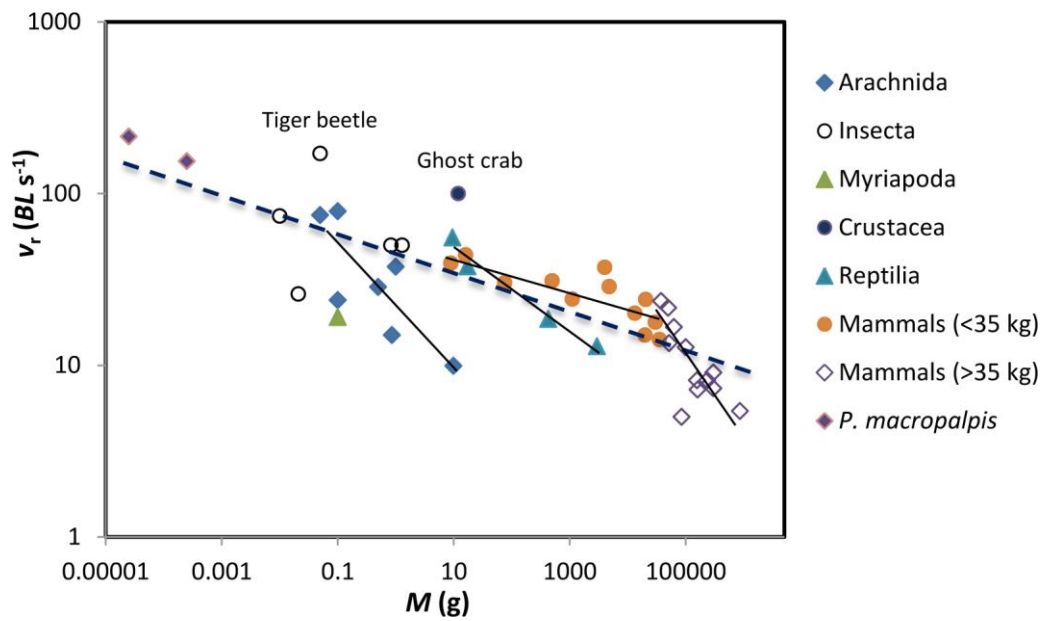


FIG. 7. Relative speed (v_r) of adult and juvenile *P. macropalpis* running in the field as a function of body mass (red diamonds) and compared to published data for other running animals. Least-squares regression lines are shown for arachnids ($\beta = -0.34$), reptiles ($\beta = -0.24$), mammals <35 kg ($\beta = 0.099$), and mammals >35 kg ($\beta = 0.42$). The dashed line shows the least-squares regression for the combined data ($\beta = 0.112$). A list of species included here, with references, is given in Appendix 2.

Appendix 1

The following analysis explains the calculation of the aerial drag force acting on the mite legs during the recovery stroke. The drag force acting on L2 and L3 was estimated assuming a mean leg velocity (u_l) of 0.4 ms^{-1} (see Figure 2), and leg length of 1.7 mm, approximating the leg as 3 cylinders with length (l) and diameter (ϕ) as shown below:



$$\begin{array}{lll} l = 0.70 \text{ mm} & l = 0.45 \text{ mm} & l = 0.55 \text{ mm} \\ \phi = 0.05 \text{ mm} & \phi = 0.03 \text{ mm} & \phi = 0.02 \text{ mm} \end{array}$$

Leg segment lengths and diameters were measured in alcohol-preserved specimens. Diameters vary from approximately 0.06 mm at the basifemur to 0.03 mm at the tibia and 0.02 mm at the tarsus. The cylinders here are modeled to approximate the dimensions of the combined basifemur, telofemur and patella (1), tibia (2) and tarsus (3).

The drag coefficient (C_D) was calculated for each of the cylinders (1, 2, 3) using the following solution for the Oseen Equation (Tomotika and Aoi, 1951): -

$$C_D = 2F' / \rho \cdot u_l^2 \cdot \phi = 8\pi / \text{Re} \cdot [0.5 - \Gamma + \ln(8/\text{Re})] \quad (6)$$

- where F' is the force per unit length on the cylinder
- ρ = density of air (1.086 kg m^{-3})
- Re = Reynolds number
- Γ = Euler's constant (0.577)

$$\text{Re} = \phi \cdot u_l / \nu \quad \text{where } \nu = \text{kinematic viscosity of air at } 325 \text{ K} = 1.807 \times 10^{-5} \text{ m}^2 \text{ s}^{-1}$$

$$\text{Re}_1 = [(5 \cdot 10^{-5} \text{ m}) (0.4 \text{ ms}^{-1}) (0.35/1.70 \text{ mm})] / (1.807 \cdot 10^{-5} \text{ m}^2 \text{ s}^{-1}) = 0.23$$

$$\text{Re}_2 = \text{Re}_1 \cdot (0.92 \text{ mm}/0.35 \text{ mm}) (0.03 \text{ mm}/0.05 \text{ mm}) = 0.36$$

$$Re_3 = Re_1 \cdot (1.425 \text{ mm} / 0.35 \text{ mm}) (0.02 \text{ mm} / 0.05 \text{ mm}) = 0.37$$

Applying these values to Equation 3, yields the following dimensionless drag coefficient (C_D) estimates for the 3 segments:

$$1 = 32 \quad 2 = 23 \quad 3 = 23$$

$$\text{Rearranging equation 3: } F' = C_D \cdot \rho \cdot u^2 \cdot \phi / 2$$

The drag force (F_i) acting on each division of the leg can then be calculated, and summed to yield an estimate of drag force (F_{total}) for the whole leg:

$$1. \quad F_1' = [(32 \text{ Nm}^{-1}) (1086 \text{ kg m}^{-3}) (0.08 \text{ ms}^{-1})^2 (5 \cdot 10^{-5} \text{ m})] / 2 = 6.9 \cdot 10^{-5} \text{ Nm}^{-1}$$

$$F_1 = (6.9 \cdot 10^{-5}) (7 \cdot 10^{-4} \text{ m}) = 4.9 \cdot 10^{-8} \text{ N}$$

$$2. \quad F_2' = [(23 \text{ Nm}^{-1}) (1086 \text{ kg m}^{-3}) ((0.4 \text{ ms}^{-1}) (0.92/1.7))^2 (2.5 \cdot 10^{-5} \text{ m})] / 2 = 4.4 \cdot 10^{-5} \text{ Nm}^{-1}$$

$$F_2 = (4.4 \cdot 10^{-5}) (4.5 \cdot 10^{-4} \text{ m}) = 2.0 \cdot 10^{-8} \text{ N}$$

$$3. \quad F_3' = [23 \text{ Nm}^{-1}) (1086 \text{ kg m}^{-3}) ((0.4 \text{ ms}^{-1}) (1.425/1.7))^2 (2 \cdot 10^{-5} \text{ m})] / 2 = 7.0 \cdot 10^{-5} \text{ Nm}^{-1}$$

$$F_3 = (7.0 \cdot 10^{-5}) (5.5 \cdot 10^{-4} \text{ m}) = 3.9 \cdot 10^{-8} \text{ N}$$

$$F_{total} = (4.9 + 2.0 + 3.9) \cdot 10^{-8} = \mathbf{1.1 \cdot 10^{-7} \text{ N}}$$

The force required to arrest the leg can be estimated using the measured deceleration of L2 and L3 (ca. 120 ms^{-2} ; Figure 2) and estimating the leg mass as $\sum(\pi \cdot (\phi/2)^2 \cdot l \cdot \rho_l)$ for the three cylinders, where l = cylinder length and ρ_l = leg density (estimated at 1100 kg m^{-3}).

$$\text{Required deceleration force} = 120 \cdot (1100 \cdot 10^3) \cdot [\pi (2.5 \cdot 10^{-5} \text{ m})^2 \cdot (7 \cdot 10^{-4} \text{ m})] + [\pi (1.5 \cdot 10^{-5} \text{ m})^2 \cdot (4.5 \cdot 10^{-4} \text{ m})] + [\pi (1 \cdot 10^{-5} \text{ m})^2 \cdot (5.5 \cdot 10^{-4} \text{ m})]$$

$$= \mathbf{2.5 \cdot 10^{-7} \text{ ms}^{-2}}$$

Appendix 2.

Relative speed and mass data for fast-running animals included in Figure 7.

Species	v_r (BL s ⁻¹)(g)	M_b	Reference
Arthropoda			
Arachnida			
Araneae			
<i>Argiope aurantia</i>	15.0	0.86	Foellmer et al., 2011
<i>Dolomedes plantarius</i>	37.5	1	Gorb and Barth, 1994 ^M
<i>Hololena adnexa</i>	24	0.1	Spagna et al., 2011 ^M
<i>Hololena adnexa</i>	79	0.1	
<i>Eratigena atrica</i>	28.6	0.5	Guinness Book
<i>Schizocosa ocreata</i>	75	0.05	Amaya et al., 2001 ^L
Solifugae			
<i>Eremobates marathoni</i>	9.9	9.9	Punzo, 1998
Acari			
<i>Paratarsotomus macropalpis</i>	154	0.00025	Rubin et al., 2015 (current study)
	214.6	0.000025	
Insecta			
<i>Formica polyctena</i>	26	0.021	Hurlbert et al., 2008
<i>Cataglyphis bombycina</i>	74	0.01	Wehner, 1983; Wittlinger et al.,
2007 <i>Periplaneta americana</i>	50	0.83	Full and Tu, 1991
<i>Onymacris plana</i>	50	1.3	Nicolson, Bartholemew & Seeley,
1984 <i>Cicindela eburneola</i>	171	0.05	Kamoun and Hogenhout, 1996
Myriapoda - Chilopoda			
<i>Scutigera coleoptrata</i>	19.1	0.1	Manton, 1965
Crustacea			
<i>Ocyropode centrophthalma</i>	100	12	Burrows and Hoyle, 1973
Reptilia			

<i>Callosaurus draconoides</i>	55.3	9.5	Irschick and Jayne, 1999
<i>Cnemidophorus tigris</i>		37.6	17.3
<i>Varanus gouldi</i>	18.6	429	Clemente et al., 2009
<i>Varanus giganteus</i>	12.9	2970	
Mammalia			
<i>Gazella thompsoni</i>	24.2	20500	
<i>Procapra gutturosa</i>	17.8	30000	See Iriate-Diaz, 2002
<i>Canis latrans</i>	20.1	13300	
<i>Vulpes fulva</i>	28.7	4800	
<i>Acinonyx jubatus</i>	15	20000	
<i>Sciurus carolinensis</i>	31.0	500	
<i>Ammospermophilus leucurus</i>	30.2	76	
<i>Neotoma lepida</i>	24.3	1100	
<i>Mus musculus</i>	43.9	16	
<i>Perognathus longimenbris</i>	39.3	8.9	
<i>Lepus europeus</i>	37.1	4000	
(larger mammals, >35 kg)			
<i>Homo sapiens</i>	5	85000	
<i>Equus zebra</i>	7.4	300000	
<i>Equus burchelli</i>	8.2	235000	
<i>Bison bison</i>	5.4	865000	
<i>Cervus elephas</i>	9.0	300000	
<i>Rangifera tarandus</i>	12.7	100000	
<i>Gazella granti</i>	16.7	62500	
<i>Antilocapra americana</i>	21.6	50000	
<i>Antilope cervicapra</i>	23.6	37500	
<i>Canis lupus</i>	14.1	35200	
<i>Panthera tigris</i>	7.2	161000	
<i>Panthera leo</i>	8.2	156000	
<i>Crocota crocuta</i>	13.5	52000	

^M = Mass estimated from other literature

^L = Length estimated from other literature



Movie 1. Pivot turn movie. Footage of *P. macropalpis* executing a pivot turn, initially in real-time and then slowed 1/30.

Table S1. Relative speed and mass data for fast-running animals included in Fig. 7

Species	v_r (BL s ⁻¹)	M_b (g)	References
Arthropoda			
Arachnida			
Araneae			
<i>Argiope aurantia</i>	15.0	0.86	Foellmer et al., 2011
<i>Dolomedes plantarius</i>	37.5	1	Gorb and Barth, 1994 ^M
<i>Hololena adnexa</i>	24	0.1	Spagna et al., 2011 ^M
<i>Hololena adnexa</i>	79	0.1	
<i>Eratigena atrica</i>	28.6	0.5	Guinness Book
<i>Schizocosa ocreata</i>	75	0.05	Amaya et al., 2001 ^L
Solifugae			
<i>Eremobates marathoni</i>	9.9	9.9	Punzo, 1998
Acari			
<i>Paratarsotomus macropalpis</i>	154	0.00025	Current study
	214.6	0.000025	
Insecta			
<i>Formica polyctena</i>	26	0.021	Hurlbert et al., 2008
<i>Cataglyphis bombycina</i>	74	0.01	Wehner, 1983; Wittlinger et al., 2007
<i>Periplaneta americana</i>	50	0.83	Full and Tu, 1991
<i>Onymacris plana</i>	50	1.3	Nicolson, Bartholemew and Seeley, 1984
<i>Cicindela eburneola</i>	171	0.05	Kamoun and Hogenhout, 1996
Myriapoda - Chilopoda			
<i>Scutigera coleoptrata</i>	19.1	0.1	Manton, 1965
Crustacea			
<i>Ocypode centrophthalma</i>	100	12	Burrows and Hoyle, 1973
Reptilia			
<i>Callosaurus draconoides</i>	55.3	9.5	Irschick and Jayne, 1999
<i>Cnemidophorus tigris</i>	37.6	17.3	
<i>Varanus gouldi</i>	18.6	429	Clemente et al., 2009
<i>Varanus giganteus</i>	12.9	2970	
Mammalia			
<i>Gazella thompsoni</i>	24.2	20,500	
<i>Procapra gutturosa</i>	17.8	30,000	See Iriate-Díaz, 2002
<i>Canis latrans</i>	20.1	13,300	
<i>Vulpes fulva</i>	28.7	4800	
<i>Acinonyx jubatus</i>	15	20,000	
<i>Sciurus carolinensis</i>	31.0	500	
	30.2	76	
<i>Ammospermophilus leucurus</i>			

Species	v_r	M_b	References
<i>Neotoma lepida</i>	24.3	1100	
<i>Mus musculus</i>	43.9	16	
<i>Perognathus longimenbris</i>	39.3	8.9	
<i>Lepus europeus</i>	37.1	4000	
(larger mammals, >35 kg)			
<i>Homo sapiens</i>	5	85,000	
<i>Equus zebra</i>	7.4	300,000	
<i>Equus burchelli</i>	8.2	235,000	
<i>Bison bison</i>	5.4	865,000	
<i>Cervus elephas</i>	9.0	300,000	
<i>Rangifera tarandus</i>	12.7	100,000	
<i>Gazella granti</i>	16.7	62,500	
<i>Antilocapra americana</i>	21.6	50,000	
<i>Antilope cervicapra</i>	23.6	37,500	
<i>Canis lupus</i>	14.1	35,200	
<i>Panthera tigris</i>	7.2	161,000	
<i>Panthera leo</i>	8.2	156,000	
<i>Crocota crocuta</i>	13.5	52,000	

^M, Mass estimated from other literature.

^L, Length estimated from other literature.